Detection and correlation analysis of seasonal vertical ground movement measured from SAR and drought conditions

Francesco Pirotti [1,2], Felix Enyimah Toffah[1,3]

[1] Dept. of Land and Agroforestry Systems (TESAF), University of Padua, Viale dell'Università 16, 35020 Legnaro, Italy – francesco.pirotti@unipd.it
[2] Interdepartmental Research Centre in Geomatics (CIRGEO), University of Padua, Viale dell'Università 16, 35020 Legnaro, Italy
[3] Dept. of Civil, Building and Environmental Engineering, Sapienza University of Rome, Via Eudossiana 18, 00184 Rome, Italy – felixenyimah.toffah@uniroma1.it

Keywords: Subsidence; drought; seasonal ground movement; SAR; Sentinel-1; Advanced Differential Interferometric Synthetic Aperture Radar (A-DInSAR)

Abstract

In this work the relationship between climatic indices and seasonal vertical ground motion (SVGM) from earth observation data is investigated. The European Ground Motion Service (EGMS) vertical ground movement measurements provided from 2018 to 2022 are used together with temperature and precipitation data from MODIS and CHIRP datasets respectively. Precipitation and temperature are further processed to provide Drought Code (DC) maps calculated ad hoc for this study at 1 km spatial resolution and daily temporal resolution. Measurement Points (MP) from EGMS over Italy provide a value of ground vertical movement approximately every 6 days. Seasonality is analysed to assess correlation between SVGM and DC from Copernicus CEMS (DC1) and from MODIS+CHIRP (DC2) and from temperature using Spearman's rank correlation coefficient (ρ). Initial results over Italy show that DC2 is significantly better correlated to SVGM than DC1 and temperature, with a stronger median absolute value of ρ of 0.025 and 0.042 respectively for negative and positive correlation scenarios. A total of 1275 MPs have correlation coefficients between DC2 map and EGMS measurements above 0.8 (positive correlation) and 2594 ρ<-0.8 (negative correlation). Correlations lagged in time are also analysed, resulting in most being inside a window of +/- 6 days. Because DC and temperature are strongly collinear, further analysis to assess which is better at explaining the seasonality of GM was carried out, resulting in DC2 significantly explaining more variance of the SVGM than temperature for the inversely correlated points more than the directly correlated points. These points are unevenly distributed in the Italian territory, with clusters in some areas that appear to show reliable SVGM-DC correlations. We conclude that further investigation is necessary at a local scale. An interactive web-gis open to the public is available for data consultation and all data are shared in a public repository for full replicability of the method.

1. Introduction

Land subsidence refers to the downward vertical displacement of the ground surface caused by natural factors such as compaction of sediments and geological processes and anthropogenic factors such as groundwater withdrawal. It leads to a reduction of the surface elevation which poses a significant threat to infrastructure, agriculture and environmental sustainability (Galloway et al., 1999). The impacts of land subsidence is exacerbated by changing climatic conditions, particularly drought conditions which are often characterised by prolonged periods of dry weather with little or no precipitation.Soils undergo notable changes in volume due to variations in soil moisture, a principle known as effective stress. During wet conditions of the soil, these soils swell, expanding their volume and exerting significant pressure on surrounding structures. Conversely, during drought conditions, there is an escape of water molecules from the soil. The soil thus desiccates and contracts which results in the lowering of the elevation of the surface (Welch et al., 2024). Consequently, the combination of land subsidence and drought conditions poses significant consequences. Understanding the interaction between ground vertical movement and drought conditions will be crucial for proactive risk management and mitigation strategies.

SAR data, acquired from satellite-based sensors, provide detailed information on ground deformation, allowing for the detection and geodetic measurement of land subsidence with unprecedented accuracy (Ferretti et al., 2007) and with high spatial and temporal resolution (Rosen et al., 2000). Interferometric SAR (InSAR) data can provide measurement of ground movements over time with millimetre precision using Pointwise Scatterers and Distributed Scatterers (Ferretti et al., 2024).

This study seeks to use Interferometric Synthetic Aperture Radar (InSAR) data derived from Sentinel-1 provided by the European Ground Motion Service (EGMS) and analyse correlations with drought code (DC) obtained from two sources: (i) the Copernicus Climate Change Service (C3S) Climate Data Store (CDS) and (ii) a 1 km resolution DC map calculated ad-hoc for this study. We aim to identify spatial and temporal patterns of land subsidence in relation to drought conditions in Italy. Drought code is part of a method to infer forest fire risk; in this study it will be used as a proxy of drought due to the fact that DC represents the condition of a layer that dries very slowly (Pirotti et al., 2023), with a time lag of approximately 52 days (Turner, 1972). This means that it reflects long-term drought conditions, which is what we assume can have significant correlation with land subsidence especially in areas of intense agricultural activity that rely on extraction of groundwater (Charpentier et al., 2022; Welch et al., 2024) and which impacts the water table. Thus, the hypothesis that we want to test in this study is that there is a correlation between land subsidence and drought conditions.

Two drought indices, described in Section 3.1.3, were used to identify spatial and temporal patterns of seasonal vertical

ground movement (SVGM) in relation to drought conditions in Italy.

To quantify the correlation between SVGM and DC, Spearman’s rank correlation coefficient will be used to assess the relationship between the two variables.

The overall goals of this work are the following:

1. To assess the spatial and temporal patterns of measurement points (MPs) monitored using A-DInSAR for seasonal vertical ground movement (SVGM) across Italy.
2. To investigate the potential correlation between SVGM and climatic conditions in Italy, examining whether drought events coincide with changes of surface elevation and ground motion patterns.
3. To identify regions within Italy where SAR-derived land subsidence and drought conditions exhibit significant spatial correlations, as well as areas with contrasting patterns.
4. To assess the implications of the identified correlation between land vertical movement and drought conditions for land management, water resource planning, and environmental sustainability.

In this work we report and discuss results primarily on the first two.

2. Materials

2.1 Study Area

This study will be limited to Italy, located in southern Europe and stretching between longitudes 6° and 19° E and latitudes 35° and 47° N. In the northern part, it is surrounded by France, Switzerland, Austria and Slovenia. The rest of the territory is surrounded by water, with the Adriatic sea to the east, the Tyrrhenian Sea to the west and the Mediterranean and Ionian seas to the south. Italy is characterised by diverse landscapes, including the Alps mountain range in the north and the Po Valley in the south. The Po Valley, one of the most significant agricultural regions is known for its fertile plains and dense urban centres.

The climate of the country is very diverse ranging from humid subtropical climate in the north to Mediterranean climate in the south. Also, there is a considerable difference in temperature between the north and the south, with the central part acting like a middle ground between the 2 zones. The north usually has a colder winter and a hot summer while the south mostly has a warmer temperature. For instance on a winter day, the extreme difference in temperature is shown when it is about -2°C and snowing in Milan (North), 8°C in Rome (central part) and 20°C in Palermo (South). This is also observed in most maps that purport to show the variation of temperature across the country. Consequently, there is an associated trend in loss of soil moisture and drought conditions across the country.

Due to the extraction of groundwater for agricultural and industrial activities in the region, as well as other factors such as tidal influence in Venice and active volcanoes in the South, land subsidence is a prominent issue (Tosi, 2019). In July 2022, there was an intense drought in Italy (Figure 1), more than what the country has experienced in the past 70 years, because of which the government declared a state of emergency over 5 regions in the Northern territory (Emilia-Romagna, Friuli-Venezia Giulia, Lombardy, Piedmont and Veneto). This happened as a result of the extreme heat which had a resulting impact on the winter snow in the region. Also, the preceding months had a low amount of recorded rain thus intensifying the drought. These make Italy a suitable area of interest for the purpose of this research activity (figure 1).

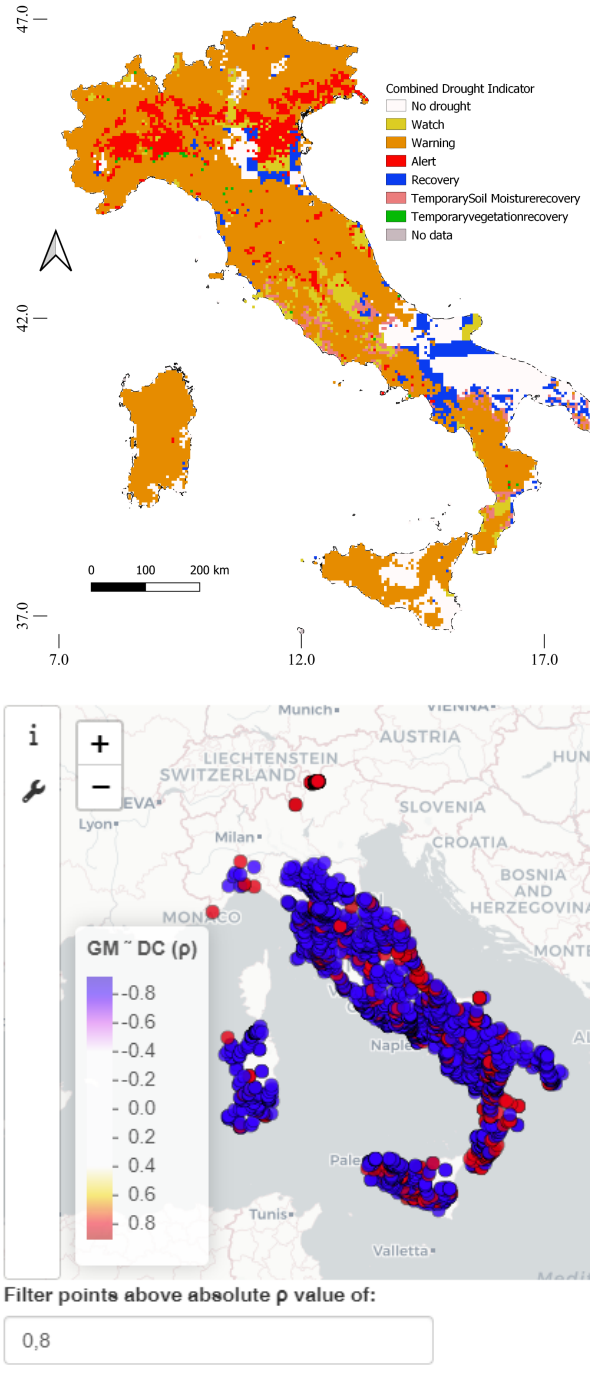

Figure 1. Top: combined Drought Indicator for Italy, first 10-day period of July 2022, (JRC, 2024); bottom: detected MPs having >0.8 absolute Spearman correlation value and accessible from the web-app developed for this study.

3. Methods

To quantify the correlation between SVGM and climatic data, the Spearman's rank correlation coefficient (ρ) was used to assess the monotonic relation between the time series of ground movement with DC values from two sources, and with temperature time-series.

3.1 Drought indices

Drought indices are tools used to quantify and monitor drought conditions by integrating weather variables, temperature and pressure of the area of interest. These indices consider rainfall deficiencies over months or even years that impact the moisture content in soils. It developed from the original Drought Index of the Canadian Danger Rating Systems (Beall, 1947). This original index was found not useful as its upper limit of 25 drying days was reached more quickly during extended drying periods. The stored moisture index (SMI) was thus developed to cater for the extended drying periods. The SMI models the variation in moisture content in upper layers of forest soil, specified by their ability to hold 8 inches of available water. The SMI is augmented by the effective rainfall, which is assumed to be the amount available for storage after interception by the canopy. This stored moisture is depleted daily by evapotranspiration and thus a transformation is applied to the SMI for evapotranspiration. To standardise with other fire weather indices, the SMI was transformed into Drought Code (DC) which is used in this study. Drought indices basically use temperature and precipitation to infer various impacts of drought on the Earth surface taking in consideration the number of drying days estimating the amount of evapotranspiration that removes moisture from the ground. Temperature and precipitation are the input variables. In this study we use daily data from satellite earth observation to infer temperature and an interpolated daily product for precipitation.

3.1.1 Air temperature estimation: the MODIS Daytime Land Surface Temperature (LST) product (MOD11A1 V6.1) was used to estimate the temperature at MPs’ positions for the intended period and calculate DC values (see equations 1-5). It must be noted that LST and air temperature are not equivalent, even if collinear, and that there are different sets of spatiotemporal characteristics that distinguish air temperature from LST (Mutiibwa et al., 2015). Using LST directly is not an ideal solution. Thus, a correction factor of 0.74 was used as the variance between LST and air temperature in accordance with the recommendation of Mutiibwa et al. (2015). It must be noted that temperature rasters have plenty of gaps in time and space due to low-quality pixels, usually from clouds or other limitations from the atmosphere or from sensor malfunctions. To fill these empty cells, a spline interpolation was applied over the 3d data cube.

3.1.2 Precipitation: an estimate of daily precipitation values were obtained from the CHIRPS dataset available on the Google Earth Engine platform. The CHIRPS dataset is a global rainfall dataset provided by the United States Geological Survey and the Climate Hazards Center. It incorporates 0.05° resolution satellite imagery (that is based on infrared Cold Cloud Duration Observations) with in-situ station data to create gridded rainfall time series using interpolation approaches (Funk et al., 2015). It is available on a daily, monthly or seasonal basis and also useful for performing trend analysis and seasonal drought monitoring making it valuable for this work. The dataset was clipped to the study area, exported and used for the analysis.

3.1.3 Drought Code (DC): Drought code is “an indicator of the moisture content in deep compact organic layers. This code represents a fuel layer approximately 10-20 cm deep. The drought code fuels have a very slow drying rate, with a time lag of 52 days. The drought code scale is open-ended, although the maximum value is about 800.” (https://www.copernicus.eu/, 2024). In this work, two versions of drought code maps are tested. One is the reanalysis grid cell resolution of 0.25° (approximately 20 km) dataset provided by Copernicus CEMS cems-fire-historical-v1 (https://www.copernicus.eu/, 2024). This will be referred to as DC1. The other version of the drought code map was computed ad-hoc with a spatial resolution of 1 km and was obtained using the precipitation and temperature datasets described in sections 3.1.1 and 3.1.2 and will be referred to as DC2. DC2 was calculated based on rainfall values from CHIRP of the day (DCt) and the DC value of the previous day (DCt−1) with the following equations:

If rainfall is equal to or above 2.8 mm:

$$DC_t = 400 \cdot \ln(800/Q_t) \quad (1)$$

$$Q_t = Q_{t-1} + 3.937 \cdot r_t \quad (2)$$

$$Q_{t-1} = 800 \cdot \exp\left(-DC_{t-1}/400\right);$$

$$r_d = 0.83 \cdot r_t - 1.27 \quad (3)$$

where:

DC_t is the drought code from rainfall data of the day, Qr is the moisture equivalent that is calculated from the moisture equivalent of the previous day, Q_t, which is in turn calculated from DC_{t-1} , i.e., the DC code of the last day, r_t is the rainfall of the day in mm from the CHIRP dataset. r_d is the amount of rain available for storage in forest soil after interception by the canopy. In case of rainfall below 2.8 mm, DC is calculated based on the temperature at mid-day and DCt−1 , i.e., the DC code of the previous day with the following equations:

$$DC_t = DC_{t-1} + 0.5 \cdot V \quad (4)$$

$$V = 0.36\,(T12 + 2.8) \cdot Lf \quad (5)$$

where T12 is the temperature at mid-day, here estimated from the MODIS LST converted to air temperature by a factor of 0.74 as documented. Lf is a day-length factor which is constant for each month and is -1.6 for the months of November through March, and 0.9, 3.8, 5.8, 6.4, 5.0, 2.4, 0.4 respectively for the months from April to October.

3.1.4 Correlation of drought with seasonal ground movement (SVGM) from Advanced Differential Interferometric Synthetic Aperture Radar (A-DInSAR): correlation was determined after first detrending for time the

ground movement from the EGMS data to remove continuous systematic subsidence or uplift over time. The goal here was to assess seasonal ground vertical motion (SVGM) and if, where and how, these measurements are related to drought recorded from the location of each MP from the EGMS. Proxies used for drought are DC1, DC2 and temperature. Spearman’s rank correlation coefficient is used for this, as it is more robust to relations which are not linear in all the range of values. Both positive and negative correlations were analysed. The former is when there is the same pattern of ground uplift with higher values of the compared variables (DC1, DC2 and temperature), the latter, viceversa, is when the ground subsides and the variable values increase. Both behaviours have been observed and documented in past scientific literature. A positive correlation, for example, is usually found when buildings have a seasonal expansion from thermal effects on the structure (Crosetto et al. 2015). In this work this is accounted for and reported, but the focus is on the negative correlations, where ground subsides from water-table depletion, which reasonably happens during prolonged periods of drought.

4. Results

At this stage the method was tested over Italy and only points that resulted in having a Spearman’s rank correlation coefficient ρ above 0.7 in its absolute value, thus denoting both strong positive and negative correlations, are extracted and further analysed. Figure 2 below shows two examples of such MPs.

4.1 Data availability and web-gis data viewer

The following three intermediate data-cube raster products and final resulting vector of points are created: (i) daily precipitation of area (mm), (ii) daily air temperature interpolated values (°C) (iii) calculated drought code (unitless) and (iv) extracted MPs with a table reporting the following attributes (see figure 3):

- Spearman’s rank correlation (ρ)
- confidence interval
- highest ρ at lagged time
- lag of higher ρ (days)

for DC1, DC2 and temperature. This latter information is seen in figure 2 below in the top row. The former, the three data-cubes, have one band per day from 1 January 2017 to 1 January 2023 for a total of 2192 bands. All are in geographic coordinate systems using the WGS84 system and aligned to an extent of 6.6116°, 18.51428°, 35.48345°, 47.09867° with a cell ground sampling distance of 8.983153×10^{-3} degrees.

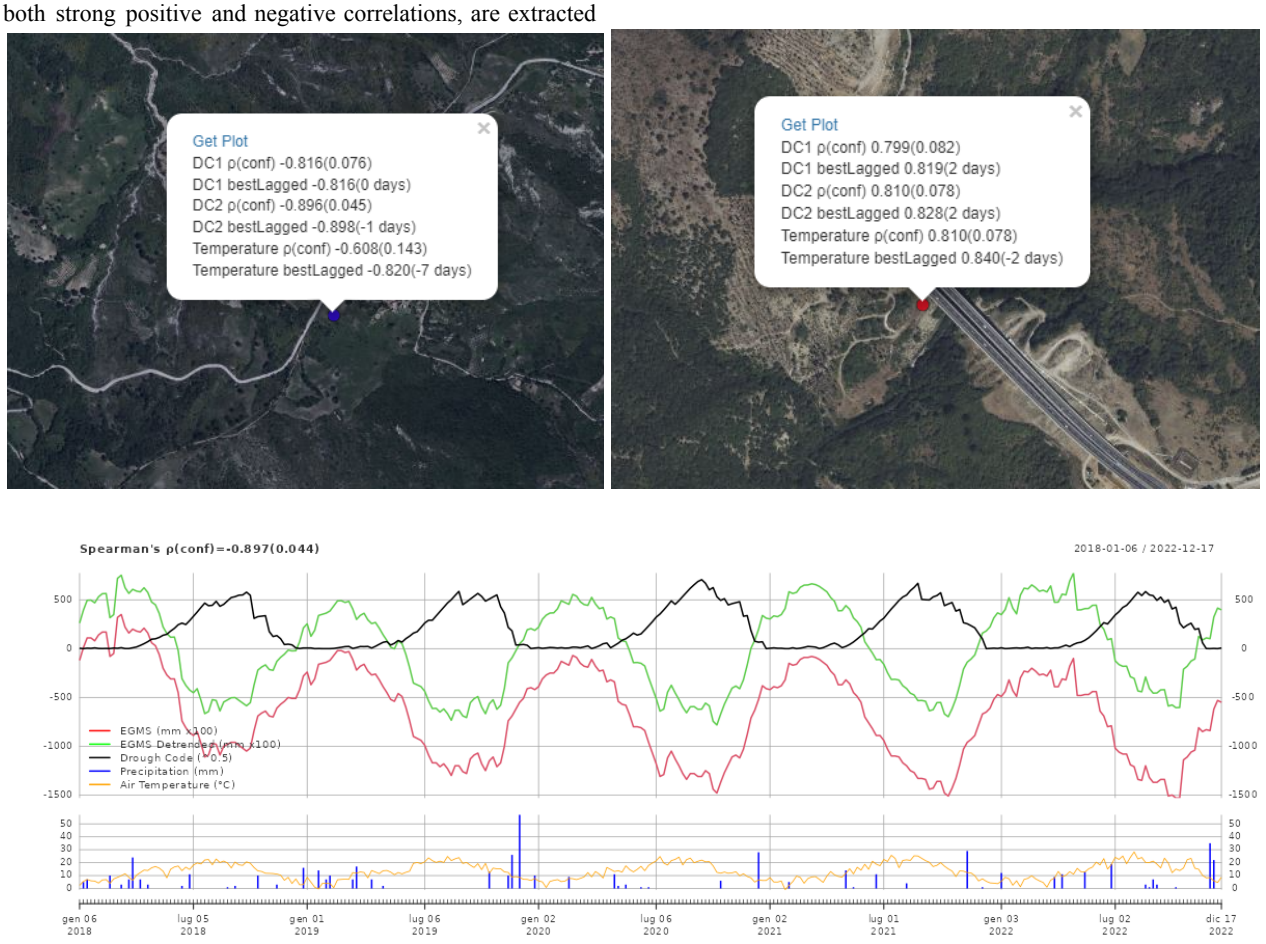

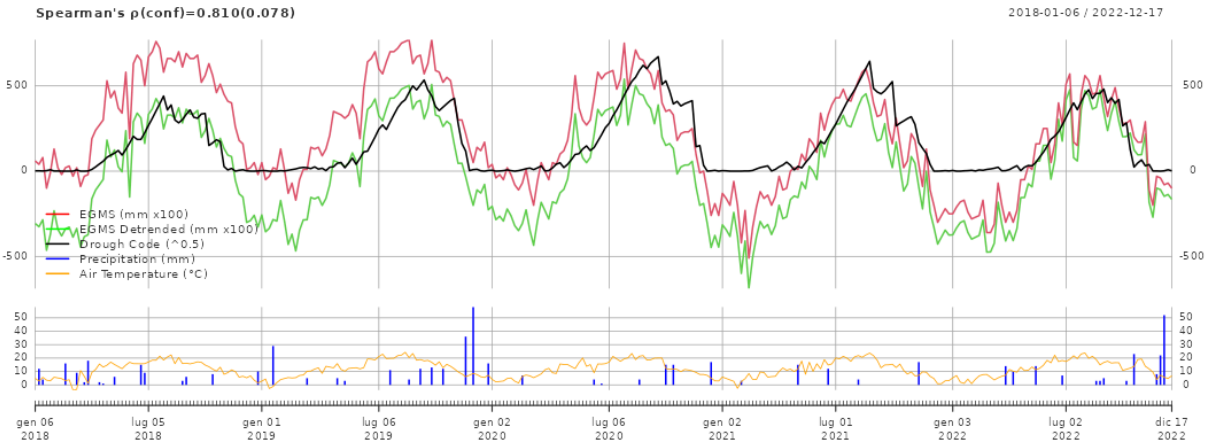

Figure 2. Climatic time-series information of two MPs with negative (top row left) and positive (top row right) Spearman correlation values. The user clicks the left mouse button over the MP to get details and a link for triggering a query over the time-series of DC2, temperature and precipitation. Middle row shows the respective plot of the top left MP with negative correlation value, and the bottom row shows the time-series plot of the top right MP with positive correlation.

All four data are available as per FAIR (Findable, Accessible, Interoperable, and Reusable) principle and are provided as open-access in Zenodo - see Pirotti, (2024) in references.

A data viewer was also developed (see Figure 1 bottom) to interact with MPs’ locations and extract and plot at each location of a single MP the time-series for temperature, precipitation, drought code and ground movement as depicted in figure 2. An example of two such queries at a random location is depicted in figure 2 where two MPs with negative (left) and positive (right) correlation are shown with respective time-series plots in middle and bottom column respectively.

4.2 A-DInSAR vertical ground movement seasonal correlations

MPs from EGMS over Italy provide a value of ground vertical movement approximately every 6 days. Results of seasonality correlated patterns using Spearman's rank correlation coefficient (ρ) between ground vertical motion measure DC1, DC2 and temperature show a significant number of points with high correlation, both negative and positive. Figure 3 shows the distribution of the ρ values.

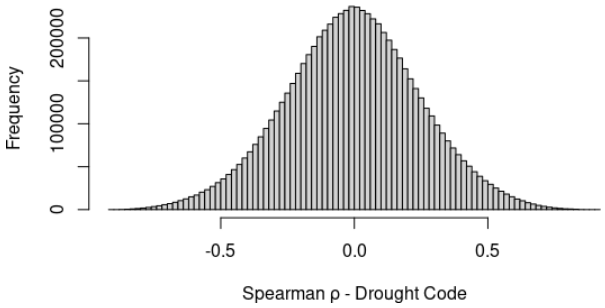

Figure 3. Histogram of frequency distribution of correlation values (ρ) at MPs.

The total number of MPs over Italy is 7 193 676. Total number of correlated points is 28 957, thus less than 0.4% (table 1). Quite clearly only a minor part of the points are correlated.

	|ρ| > 0.7	**|ρ| > 0.8**
negative ρ	18 090	2 594
positive ρ	10 867	1 275
total	**28 957**	**3 869**

Table 1. Number of MPs with strong correlation between SVGM and DC2.

From table 1 above it can be seen that a total of 1275 MPs have positive correlation coefficients between DC2 map and EGMS measurements above 0.8 and 2594 have ρ below -0.8 (negative correlation). Correlations lagged in time are also analysed, resulting in most of the correlated MPs having stronger correlation at the day for which they were calculated (0 days lag time - figure 4).

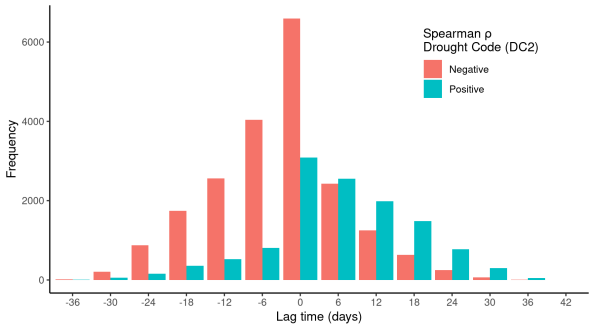

Figure 4. Lag-time distribution of best correlations between DC2 and vertical ground motion.

The above observation does not hold true for temperature, where important lag times improve the correlation

significantly. Figure 5 shows that a month's negative lag time give the best correlation for negatively correlated MPs.

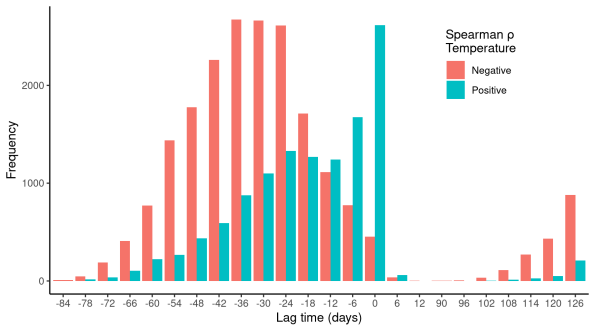

Figure 5. Lag-time distribution of best correlations between temperature derived from calibrated MODIS and vertical ground motion .

4.2.1 DC1 vs DC2: initial results over Italy show that DC2 is significantly better correlated to SVGM than DC1, with a stronger median absolute value of ρ of 0.025 and 0.042 respectively for negative and positive correlation scenarios. Figure 6 below, on the left column, shows this difference as the scatter points are mostly on the right of the 1:1 diagonal line for negative correlation and viceversa on positive correlation. This means that most points with negative correlation regarding ground motion patterns with respect to DC, show that, for DC2-DC1 pairs, DC2 is usually more negative (stronger negative correlation). The opposite is true for positive correlation scenarios. Kruskal-Wallis pairwise difference of medians provides a p-value of significant difference <0.001.

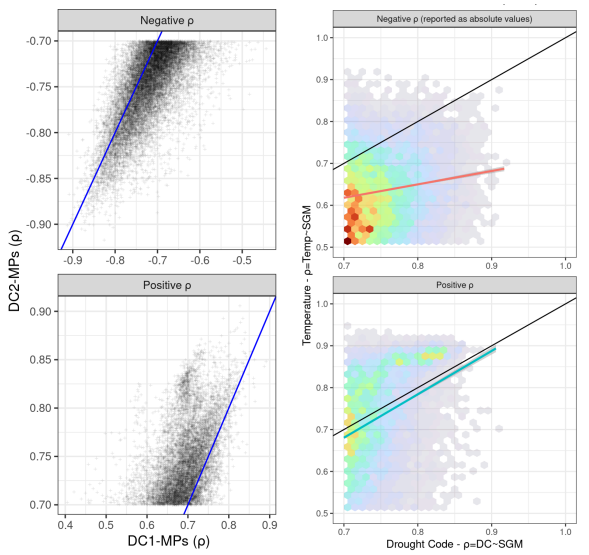

Figure 6. Left column shows pairwise DC1-DC2 values of correlations with ground motion; the right column shows temperature vs DC2 correlation. Top and bottom rows are negative and positive ρ values from testing correlation with vertical ground motion

4.2.2 DC and temperature: because DC and temperature are strongly collinear, further analysis to assess which is better at explaining the seasonality of ground motion was carried out. Results shown in figure 6 on right column show that DC2 significantly explains more variance than temperature if we consider negative correlation. Positive correlation with SVGM has mixed components, but mostly seem to be temperature driven.

4.2.3 MPs spatial distribution: MPs with high correlations with SVGM patterns points are unevenly distributed in the Italian territory, with clusters in some areas that appear to show reliable SVGM-DC correlations. In particular figure 1 bottom shows how the north-eastern part of Italy has many gaps with respect to the rest of the territory. More investigation will be needed to understand the causes. Correlated vertical movement with either temperature or DC2 should be separated to divide different dynamics. There are probably different phenomena being entangled, such as the thermal expansion of infrastructure together with subsidence from water table depletion.

5. Discussion

We compare correlations between two DC values, one from Copernicus at 20 km cell ground sampling distance and one calculated from MODIS and CHIRP. Figure 2 shows an example of two locations with clear correlations between detrended GM (green line) and DC2 (black line). It is worth noting that the EGMS data have a grid with nodes potentially every 100 m, whereas the DC2 grid has nodes every 1 km, thus more EGMS points can fall inside a single DC2 cell. In this work we managed to provide daily drought code maps (DC2) at 1 km resolution thanks to the MODIS data. Downscaling to higher resolution to match the EGMS resolution might be possible by applying methods available in literature (Abdollahipour et al. 2022). Further correlations .

5.1 Initial considerations

Each EGMS tile consists approximately of 150 000 measurement points; we tested 92 tiles that cover Italy. Each measurement point is a time-series of displacement values measured approximately every 6 days, for the years available from EGMS, 2018-2022, so 5 years, therefore about 300 observations for each MP. The corresponding DC values were extracted at each point using the Copernicus CEMS data (DC1) with 0.25° GSD and our own data calculated from MODIS and CHIRP (DC2) and the corrected temperature values from MODIS. The Spearman rank correlation was calculated, along with a confidence interval to assess the correlation with seasonal patterns of ground vertical movement. Vertical ground movement measured values were detrended to keep only seasonal variations and not linear trends of sinking or raising terrain. Analysis of lagged correlations show other interesting aspects, such as the temperature correlating with vertical movement in many points after a month time over negatively correlated points, suggesting that a drying period affects the results.

There is a strong connection between drought and temperature. High temperatures can increase evaporation rates, which increase the drought effects by drying out the soil and reducing available water. Climate change is also expected to increase the frequency and intensity of droughts in many parts of the world, due to rising temperatures. For the above reasons, understanding more the effects that it can have on the vertical ground movement can help monitoring cause and effects. This should be taken into consideration as negatively correlated points will reasonably be affected.

Other specific cases worth noting include the one in figure 7 below.

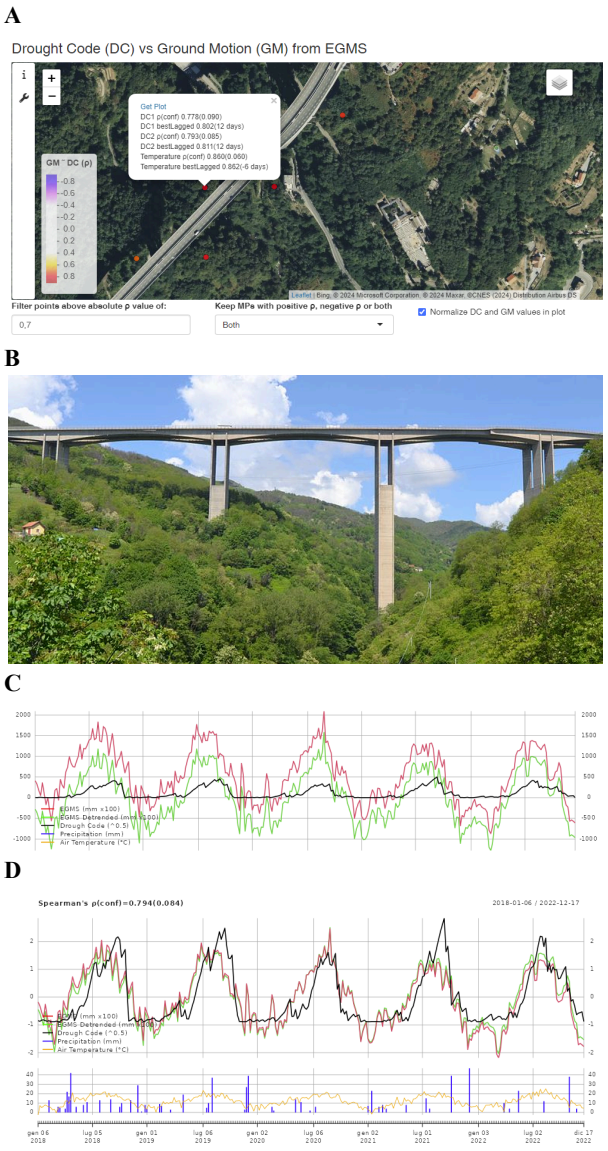

Figure 7. Temperature-driven vertical movement of road infrastructure. Top window (A) the MP, (B) a side view of the bridge, (C) time-series of vertical movement values (D) normalized values of vertical movement and temperature.

Of course these correlations are region-specific. They depend on the type of infrastructure and specific dynamics. More complex phenomena can derive from more complex combinations of geological structure of the area, and water incoming from sea level rise or other dynamics (Kanan et al., 2023). One technology that can validly provide vertical movement information is laser scanning from aerial platforms (e.g. aerial laser scanning, ALS) or terrestrial laser scanning from fixed stations that provide the deformation data to correlate with other variables.

5.2 Collinearity between drought codes and temperature

The outcome of this research can contribute to the development of effective mitigation strategies and sustainable land management practices in the face of changing climatic conditions. Understanding patterns of vertical land movement is key for monitoring the Environment in heavily urbanised areas in Europe and in the globe.

One observation related to the DC is that it might be worth assuming that a more specific index that better correlates with seasonal ground movement patterns can be created. This will be the objective of further studies. Another future work will be the replication of this study over all of Europe, to use all of the EGMS dataset for this analysis.

In this case we see a positive Spearman correlation value for temperature of ρ=0.860, higher than the one from DC2 (ρ=0.793). We have already noted that positive correlations are more driven from temperature; figure 6 on the right-bottom plot panel shows that temperature correlations are higher (above the black 1:1 line). This is evident in figure 7 as it is a very high bridge “Viadotto Gorsexio” with a central pillar taller than 172 m. Thermal deformation from temperature is quite well known (Qin et al. 2018) and our results provide further evidence that open-data can be used to monitor infrastructure seasonal movement.

Since we can prove that temperature affects the vertical dynamics of bridges, we can further provide means for monitoring these infrastructures using InSAR values. The fact that here we have a value every 6 days is a limit, but this can be overcome by future earth observation investments. Let’s think about a daily monitoring of infrastructure using daily passes of SAR satellites. This can be a valid motivation for further research and investment in development of sensors and satellite platforms.

6. Conclusions

From this work the following conclusions can be summarized:

- DC2 data cube at 1 km resolution with daily DC values created ad hoc (Pirotti 2024) for this work correlates better with MPs’ seasonal patterns of vertical movement than the DC1 from Copernicus CEMS, both for positive and negative correlations. This is unsurprising as DC2 has a better spatial resolution than DC1.
- Lag time analysis on DC2-SVGM correlation shows that DC2 well catches the time-frame for the effects of drought conditions on ground vertical movement with negative correlation. Thus this index can validly show how ground level sinks when drought conditions increase and viceversa.
- Temperature alone does not explain SVGM patterns as well as DC2, but it does provide important information on specific locations relative to infrastructure (figure 7).

Further analysis is foreseen to scale to a pan-European map of MPs that are affected by drought conditions.

Furthermore casualties at locations must also be further investigated, to understand what is the direct driver of the vertical seasonal moment.

Acknowledgements

This study was carried out within the Agritech National Research Center and received funding from the European Union Next-GenerationEU (PIANO NAZIONALE DI RIPRESA E RESILIENZA (PNRR) – MISSIONE 4 COMPONENTE 2, INVESTIMENTO 1.4 – D.D. 1032 17/06/2022, CN00000022). This manuscript reflects only the authors’ views and opinions, neither the European Union nor the European Commission can be considered responsible for them.

References

Abdollahipour, A., Ahmadi, H., Aminnejad, B., 2022. A review of downscaling methods of satellite-based precipitation estimates. *Earth Sci Inform* 15, 1–20. https://doi.org/10.1007/s12145-021-00669-4

Beall, H.W. 1947. Canadian Forest Fire Danger Rating System. Information Report FF-X-8.

Bokhari, R., Shu, H., Tariq, A., Al-Ansari, N., Guluzade, R., Chen, T., Jamil, A., Aslam, M., (2023), ‘Land Subsidence Analysis Using Synthetic Aperture Radar Data’, *Heliyon*, Volume 9, Issue 3.

Copernicus Emergency Management Service, 2019. Fire danger indices historical data from the Copernicus Emergency Management Service. In: Copernicus Climate Change Service (C3S) Climate Data Store (CDS). Copernicus Programme, Brussels, Belgium

Charpentier, A., James, M., and Ali, H.: 2022. Predicting drought and subsidence risks in France, *Nat. Hazards Earth Syst. Sci.*, 22, https://doi.org/10.5194/nhess-22-2401-2022

Crosetto, M., Monserrat, O., Cuevas-González, M. Devanthéry, N., Crippa, B., 2016. Persistent Scatterer Interferometry: a review. *ISPRS Journal of Photogrammetry and Remote Sensing*, 115, 78-89.

Crosetto, M., Monserrat, O., Cuevas-González, M., Devanthéry, N., Luzi, G., Crippa, B., 2015. Measuring thermal expansion using X-band persistent scatterer interferometry. *ISPRS Journal of Photogrammetry and Remote Sensing* 100, 84–91. https://doi.org/10.1016/j.isprsjprs.2014.05.006

Ferretti, A., E. Passera, and R. Capes. 2021. End-to-End Implementation and Operation of the European Ground Motion Service (EGMS): Algorithm Theoretical Basis Document. Technical Report EGMS-D3-ALG-SC1-2.0-006. 2021. Available online: https://land. copernicus. eu/user-corner/technical-library/egms-algorithm-theoretical-basis-document (accessed on 10 April 2024).

Mutiibwa, D., Strachan, S., Albright, T., 2015. Land Surface Temperature and Surface Air Temperature in Complex Terrain. I*EEE Journal of Selected Topics in Applied Earth Observations and Remote Sensing* 8, 4762–4774. https://doi.org/10.1109/JSTARS.2015.2468594

Kanan, A.H., Pirotti, F., Masiero, M., Rahman, M.M., 2023. Mapping inundation from sea level rise and its interaction with land cover in the Sundarbans mangrove forest. Climatic Change 176, 104. https://doi.org/10.1007/s10584-023-03574-5

Pirotti, F., Adedipe, O., Leblon, B., 2023. Sentinel-1 Response to Canopy Moisture in Mediterranean Forests before and after Fire Events. *Remote Sensing* 15, 823. https://doi.org/10.3390/rs15030823

Pirotti, F. 2024. Temperature, precipitation and drought code at 1 km resolution over Italy from start of 2017 to end of 2022 (6 years) [Data set]. Zenodo https://doi.org/10.5281/zenodo.12741043

Qin, X., Zhang, L., Yang, M., Luo, H., Liao, M., Ding, X., 2018. Mapping surface deformation and thermal dilation of arch bridges by structure-driven multi-temporal DInSAR analysis. *Remote Sensing of Environment* 216, 71–90. https://doi.org/10.1016/j.rse.2018.06.032

Raspini, F., Caleca, F., Soldato, M. D., Festa, D., Confuorto, P., Bianchini, S. (2022), ‘Review of Satellite Radar Interferometry for Subsidence Analysis’, *Earth-Science Reviews*, Volume 235, 39pp, https://doi.org/10.1016/j.earscirev.2022.104239.

Tosi, L., (2019), ‘Land subsidence in italy: from a few well-known case studies in the past to several almost unknown occurrences at present’, *Workshop for Land Subsidence Prevention*, 14th May 2019, Institute of Geosciences and Earth Resources – National Research Council, Italy, 23pp.

Turner, J.A. 1972. The Drought Code Component of the Canadian Forest Fire Behaviour System; Canadian Forestry Service Headquarters: Ottawa, ON, Canada; p. 5.

Wagner, C.E.V., 1974. Structure of the canadian forest fire weather index. *Canadian Forestry Service* 1333.